Sign Change of Hyperpolarizabilities of Solvated Water, Revised: Effects of Equilibrium and Nonequilibrium Solvation†

Kristian O. Sylvester-Hvid,*,‡ Kurt V. Mikkelsen,‡,§ Patrick Norman,⊥ Dan Jonsson,#,¶ and Hans Ågren#

Department of Chemistry, H. C. Ørsted Institute, University of Copenhagen, DK-2100 Copenhagen Ø, Denmark, Institute of Physics and Measurement Technology, Linköping University, S-58183, Linköping, Sweden, and Laboratory of Theoretical Chemistry, AlbaNova University Center, Royal Institute of Technology, S-106 91, Stockholm, Sweden

Received: March 23, 2004; In Final Form: July 7, 2004

The second harmonic and electro-optical responses for the water molecule in its liquid state are theoretically revised. The continuum, semicontinuum, and supermolecular solvation models are employed using quadratic response theory at the Hartree−Fock level, either in the equilibrium or nonequilibrium implementation. The experimentally observed sign change of the second harmonic response of water on liquefaction is reproduced using the supermolecular and semicontinuum model for both equilibrium and nonequilibrium solvation. The conclusions of a previous study, which rested upon linear response theory in an equilibrium implementation, are confirmed. Also, the assumption of Kleinman symmetry and dispersion is addressed.

Introduction and Motivation

This article is devoted to the second harmonic generation (SHG) response for water in the gas and liquid phases, respectively. Experimentally, it has been established that this property changes sign going from the gas into the liquid phase. Using the EFISH technique, Levine et al.[1] measured the SHG response for liquid water and estimated the contribution from $\beta_{\|}(-2\omega;\omega,\omega)$ to be $(8.3 \pm 1.2) \times 10^{-32}$ esu at 1064 nm. For water in the gas phase Ward et al.,[2] using the same technique, estimated $\beta_{\|}$ to $(-9.5 \pm 0.8) \times 10^{-32}$ esu at 694.3 nm, and later Kaatz et al.[3] obtained $(-8.3 \pm 0.8) \times 10^{-32}$ esu at 1064 nm. Here, as in the rest of this paper, we comply with the B-convention in discussing the magnitude of β.[4] In a previous contribution by some of us,[5] this particular sign change was given a theoretical justification, but recent developments in solvent models now render a revision appropriate.

The attention given the optical properties of water by experimentalists, is currently matched by an increasing theoretical interest for water in its different phases. For our part, in the development of theoretical solvation models using ab initio electronic structure methods, water has been an appropriate choice of benchmark molecule. The benefit of focusing on water is that the vacuum molecule has been investigated theoretically, using various high-level electronic structure methods. Thus a certain confidence level with regard to choice of method has been established. Also, the small size of the water molecule, besides making gas-phase experiments feasible, makes ab initio computations on small assemblies of water molecules possible. In the sense that such computations serve as one entry to solvent models, i.e., the supermolecular models, it is intriguing that some experiments are indicative of a microstructure in the liquid phase of water, resembling that of ice.[6] Moreover, spectroscopically, water is characterized by a high-energy first electronic absorption giving a broad window of optical frequencies within which optical processes can be studied elastically.

On the other hand, the theoretical description of liquid water is very challenging because several types of molecular interactions characterize the condensed phase. In fact, no solvation model to date offers a unified and correct description of the optical properties for highly polar (and associated) liquids, such as water. The inherent problem is obviously mastering a unified description of processes on very different time scales. Typically, models addressing translational, rotational, and vibrational degrees of freedom provide qualitative correct results for the low-frequency limit, but subsequently fail at optical frequencies. Conversely, solvent models based on electronic structure methods give no account of the low-frequency dynamics. Our solvent model belongs to the latter category and although we have the facilities to model molecular interactions, we inevitably probe only the electronic contribution to various optical properties.

In previous investigations by some of us, solvation was modeled using the equilibrium multiconfigurational self-consistent reaction field (MCSCRF)[7] continuum model for monomeric water. Later effects of a first solvation shell were specifically accounted for by supermolecular and semicontinuum computations.[5] Using finite field methods dynamic polarizabilities, $\alpha(-\omega;\omega,E)$, were obtained and used to derive electro-optical (EO) coefficients, $\beta(-\omega;\omega,0)$. Based upon these, conclusions regarding the dipolar SHG response, $\beta_{\|}(-2\omega;\omega,\omega)$ were drawn: the continuum model failed to reproduce the sign change of $\beta_{\|}(-2\omega;\omega,\omega)$ upon liquefaction, whereas the supermolecular model gave the correct sign change. Only with the semicontinuum model was a quantitative correct description of $\beta_{\|}(-2\omega;\omega,\omega)$ obtained in terms of sign and magnitude, however.

Our primary focus with the present revision is to question if the above conclusion remains valid when the proper third-order

† Part of the "Gert D. Billing Memorial Issue".

* Corresponding author. E-mail: ksh@theory.ki.ku.dk. www.sylvester-hvid.dk/kristian.

‡ University of Copenhagen.

§ E-mail: kmi@theory.ki.ku.dk.

|| Linköping University.

⊥ E-mail: panor@ifm.liu.se.

AlbaNova University Center.

¶ E-mail: dj@physto.se.

10.1021/jp048697o CCC: $27.50
Published on Web 08/31/2004

response properties are derived, and additionally when the nonequilibrium solvation is accounted for.[8−10] From preliminary studies of the water monomer we established that equilibrium solvation exaggerates the magnitude of β.[10] Also, conclusions based on the EO coefficients are only indicative of the SHG response, especially if Kleinman symmetry is assumed. Employing our implementation of the quadratic solvent response method,[10] these points of criticism are eliminated. Also, we perform more consistent computations with respect to the choice of basis set and molecular orientation and point out misprints in the previous contributions.

There have been several recent theoretical investigations of the first hyperpolarizability of the water molecule in the condensed phase. The coupled cluster/dielectric continuum model at the CC2 and CCSD level, adopted in both the equilibrium and nonequilibrium approach, was used to account for the sign change of $\beta_{||}$.[11] In the discrete solvent reaction field approaches, bulk water is partitioned into a quantum mechanical (QM) system (the water monomer) and a remaining classical molecular mechanics (MM) system. Such QM/MM approaches have been used in the computation of $\beta_{||}$ for the solvated water molecule at the MCSCF,[12] CC(CC2,CCSD),[11] and DFT[13] levels of theory. Representing the surrounding MM system in terms of electric dipolar fields perturbing the QM system has also been used[14,15] as well as a charge perturbation variant of the finite field method.[16] In the latter case only the static contribution to $\beta_{||}$ was derived, however.

Methods and Computations

We employ the continuum, semicontinuum, and supermolecular approaches in the study of water solvated by water and draw comparisons with the gas-phase description. For reasons of consistency in comparing different solvation models, all computations in this study were performed using the same geometry for the individual water unit, namely: $r_{OH} = 0.958\,019$ au and $\theta_{HOH} = 104.50$. Similar remarks apply for the choice of basis set: this consisted of 10s6p3d GTOs contracted to 5s3p2d on oxygen and 6s4p GTOs contracted to 3s1p on hydrogen, corresponding to 36 CGTOs in a monomer computation using a spherical harmonic basis. The cutoff for integral evaluation was 10^{-15} au and further details regarding contraction coefficients are found in ref 17. All computations were performed at the Hartree−Fock (HF) level, and the linear and quadratic response equations were solved at the four input frequencies: ω_i = (0.0000, 0.0345, 0.0656, and 0.0932) au, to yield $\boldsymbol{\alpha}(-\omega_i;\omega_i)$, $\boldsymbol{\beta}(-2\omega_i;\omega_i,\omega_i)$, and $\boldsymbol{\beta}(-\omega_i;\omega_i,0)$.

The water monomer was studied in the continuum SCRF approach with the water molecule having its center of mass at the origin of the spherical cavity of radius 4.00 au. C_{2v} symmetry was used with a molecular orientation corresponding to the molecular plane coincident with the *xz*-plane and the dipole moment along the *z*-axis; see the central water molecule in Figure 1. Equilibrium solvation was modeled by a dielectric medium with $\epsilon = 78.54$ and nonequilibrium solvation by a medium with $\epsilon_{st} = 78.54$ and $\epsilon_{op} = 1.78$, the latter value obtained from the refractive index of water. The multipolar expansion of the reaction field was truncated at $l = 9$. In Tables 1 and 2 we list $\boldsymbol{\beta}(-\omega;\omega,0)$ and $\boldsymbol{\beta}(-2\omega;\omega,\omega)$, respectively, obtained for these computations along with the corresponding gas-phase results.

The supermolecular approach was used to model solvent effects due to the strong hydrogen-bonding structure in the liquid phase. Indications of such a microstructure come from both neutron diffraction studies[6] and molecular dynamics (MD) studies[18−20] of liquid water. The diffraction studies indicate that, upon melting, some *local* structure characteristic of ice prevails. From the MD studies such microstructure is understood in terms of consecutive solvation shells. Therefore, as a first approximation, it seems reasonable to represent the first solvation shell in liquid water with the nearest neighbor configuration, as observed in ice.[6] As the supermolecule we thus use the water pentamer shown in Figure 1 (the central monomer and its solvation shell), characterized by two ingoing and two outgoing hydrogen bonds, and with the appropriate C_{2v} symmetry of the central monomer.

We obtain the molecular response properties of the central water molecule by subtraction of corresponding extensive properties obtained from computations on the pentamer and the

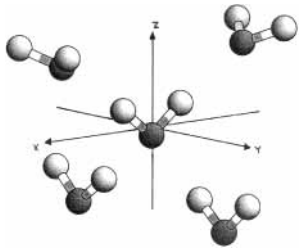

Figure 1. Pentameric water cluster consisting of the central water molecule and the first solvent shell. The structure is an idealization of the local structure for ice[6] such that the C_{2v} symmetry of the monomer is preserved. Gray spheres correspond to the oxygen atoms and white spheres to the hydrogen atoms. Coordinates are available upon request.

TABLE 1: $\boldsymbol{\beta}(-\omega;\omega,0)$ (au) As Derived in the Continuum Model for Solvation of the Water Monomer[a]

ω (au)	β_{zzz}	β_{xxz}	β_{zxx}	β_{yyz}	β_{zyy}
		$\epsilon = 1.00$			
0.0000	−1.806	−5.262	−5.262	0.136	0.136
0.0345	−1.846	−5.315	−5.319	0.085	0.133
0.0656	−1.956	−5.459	−5.475	−0.063	0.125
0.0932	−2.124	−5.672	−5.706	−0.310	0.112
		$\epsilon = 78.54$			
0.0000	1.584	−5.557	−5.557	1.899	1.899
0.0345	1.591	−5.610	−5.609	1.880	1.926
0.0656	1.609	−5.751	−5.750	1.825	1.999
0.0932	1.635	−5.960	−5.959	1.727	2.111
		$\epsilon_{st} = 78.54$ and $\epsilon_{op} = 1.778$			
0.0000	1.284	−3.748	−3.748	1.364	1.364
0.0345	1.289	−3.781	−3.780	1.347	1.382
0.0656	1.304	−3.871	−3.869	1.299	1.431
0.0932	1.324	−4.004	−3.999	1.216	1.507

[a] The cavity radius is 4.00 au and the gas-phase limit is reached for $\epsilon = 1.00$.

TABLE 2: $\boldsymbol{\beta}(-2\omega;\omega,\omega)$ (au) As Derived in the Continuum Model for Solvation of the Water Monomer[a]

ω (au)	β_{zzz}	β_{xxz}	β_{zxx}	β_{yyz}	β_{zyy}
		$\epsilon = 1.00$			
0.0345	−1.930	−5.429	−5.442	0.025	0.177
0.0656	−2.302	−5.908	−5.966	−0.357	0.309
0.0932	−2.985	−6.704	−6.872	−1.264	0.585
		$\epsilon = 78.54$			
0.0345	1.605	−5.717	−5.716	1.887	2.028
0.0656	1.660	−6.172	−6.174	1.822	2.424
0.0932	1.737	−6.913	−6.948	1.601	3.168
		$\epsilon_{st} = 78.54$ and $\epsilon_{op} = 1.778$			
0.0345	1.300	−3.849	−3.847	1.347	1.455
0.0656	1.344	−4.136	−4.130	1.278	1.734
0.0932	1.406	−4.600	−4.605	1.076	2.254

[a] The cavity radius is 4.00 au and the gas-phase limit is reached for $\epsilon = 1.00$.

TABLE 3: $\beta(-\omega;\omega,0)$ (au) As Derived Using the Semicontinuum Model with a Cavity Radius of 8.73 au[a]

ω (au)	β_{zzz}	β_{xxz}	β_{zxx}	β_{yyz}	β_{zyy}
		$\epsilon = 1.00$			
0.0000	2.084	-0.950	-0.950	7.715	7.715
0.0345	2.092	-0.952	-0.982	7.776	7.792
0.0656	2.112	-0.954	-1.072	7.938	8.002
0.0932	2.144	-0.951	-1.214	8.169	8.315
		$\epsilon = 78.54$			
0.000	10.476	2.183	2.183	13.568	13.568
0.0345	10.609	2.247	2.197	13.713	13.733
0.0656	10.971	2.430	2.234	14.103	14.184
0.0932	11.521	2.732	2.286	14.682	14.863
		$\epsilon_{st} = 78.54$ and $\epsilon_{op} = 1.778$			
0.000	8.223	2.254	2.254	11.300	11.300
0.0345	8.322	2.312	2.270	11.415	11.432
0.0656	8.589	2.476	2.311	11.724	11.789
0.0932	8.995	2.744	2.370	12.181	12.327

[a] For $\epsilon = 1.00$ the supermolecular approach is retrieved.

TABLE 4: $\beta(-2\omega;\omega,\omega)$ (au) As Derived Using the Semicontinuum Model with a Cavity Radius of 8.73 au[a]

ω (au)	β_{zzz}	β_{xxz}	β_{zxx}	β_{yyz}	β_{zyy}
		$\epsilon = 1.00$			
0.0345	2.107	−0.986	−1.081	7.917	7.969
0.0656	2.179	−1.089	−1.501	8.476	8.722
0.0932	2.349	−1.270	−2.381	9.339	10.064
		$\epsilon = 78.54$			
0.0345	10.884	2.331	2.174	14.032	14.098
0.0656	12.102	2.821	2.111	15.371	15.678
0.0932	14.313	3.911	1.861	17.640	18.528
		$\epsilon_{st} = 78.54$ and $\epsilon_{op} = 1.778$			
0.0345	8.525	2.390	2.258	11.668	11.721
0.0656	9.421	2.834	2.240	12.725	12.972
0.0932	11.033	3.793	2.095	14.501	15.213

[a] For $\epsilon = 1.00$ the supermolecular approach is retrieved.

empty solvent shell (tetramer). This we refer to as the differential shell approach.[5]

The semicontinuum approach was realized by repeating the above supermolecular computations, but now in the context of the equilibrium and nonequilibrium SCRF solvation model. All parameters were the same as for the monomer continuum computations, except for the cavity radius: to accommodate space for the first solvation shell in the cavity of the dielectric medium (the outer solvent), the cavity radius was extended to 8.73 au (and not 8.01 au which is a misprint in ref 5). Again, molecular properties for the monomer were obtained by the differential shell approach. Results of these semicontinuum computations are shown in Tables 3 and 4 for $\boldsymbol{\beta}(-\omega;\omega,0)$ and $\boldsymbol{\beta}(-2\omega;\omega,\omega)$, respectively, along with results for the corresponding supermolecular computations ($\epsilon = 1.0$).

Finally, we have evaluated the components of $\boldsymbol{\beta}(-\omega;\omega,0)$ and $\boldsymbol{\beta}(-2\omega;\omega,\omega)$ along a static electric field in the *z*-direction according to

$$\beta_{\parallel} = \frac{1}{5}\sum_{i=x,y,z}(\beta_{zii} + \beta_{iiz} + \beta_{izi}) \qquad (1)$$

which in the case of $\boldsymbol{\beta}_{\parallel}(-2\omega;\omega,\omega)$ can be compared with the dipolar contribution from the EFISH experiment. In Figures 2 and 3 we compare the dispersion of $\beta_{\parallel}(-\omega;\omega,\omega)$ and $\beta_{\parallel}(-2\omega;\omega,0)$, respectively, among the different solvation models employed and to that of the corresponding gas-phase results.

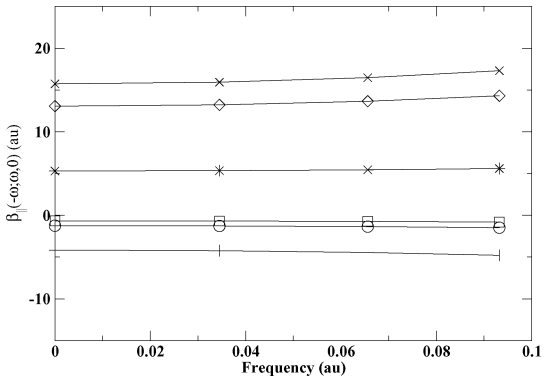

Figure 2. Dispersion of $\beta_{\parallel}(-\omega;\omega,0)$ (au) as derived within the different solvent models along with the vacuum result: (×) equilibrium semicontinuum solvation; (◇) nonequilibrium semicontinuum solvation; (∗) supermolecular model; (□) nonequilibrium continuum solvation; (⊙) equilibrium continuum solvation; (+) gas-phase water molecule.

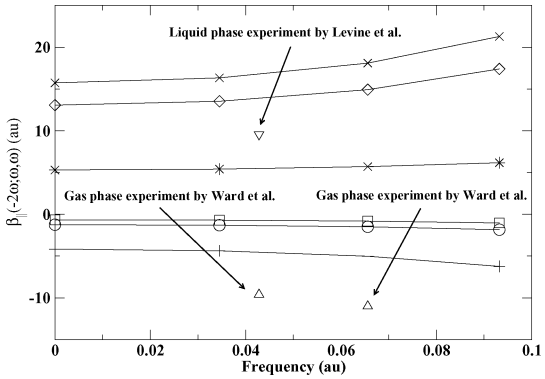

Figure 3. Dispersion of $\beta_{\parallel}(-2\omega;\omega,\omega)$ (au) as derived within the different solvent models along with the vacuum result and experimental values: (×) equilibrium semicontinuum solvation; (◇) nonequilibrium semicontinuum solvation; (∗) supermolecular model; (□) nonequilibrium continuum solvation; (⊙) equilibrium continuum solvation; (+) gas-phase water molecule; (△) gas-phase experiment at 694.3 nm by Ward et al.[2] and at 1064 nm by Kaatz et al.;[22] (▽) liquid-phase experiment at 1064 nm by Levine et al.[1] Experimetal values converted according 1 β (au) = 8.6392×10^{-33} esu.

Although the effect of electron correlation on β for water is generally acknowledged,[5,10,21] here we restricted all computations to the HF level due to lack of size extensivity in the MCSCF procedure and ambiguities in choosing consistent complete active spaces for the structures investigated.

Results

In this section we discuss the results for the EO ($\boldsymbol{\beta}^{\omega}$) and SHG ($\boldsymbol{\beta}^{2\omega}$) effect as presented in Tables 1−4. Unless otherwise stated, we discuss the two effects under one heading ($\boldsymbol{\beta}$) because the various components of $\boldsymbol{\beta}^{2\omega}$ and $\boldsymbol{\beta}^{\omega}$ are quite similar. Therefore, already at this point we can validate one assumption made in previous work: evaluation of $\boldsymbol{\beta}^{\omega}$ within the different solvation models does give a qualitative understanding of the corresponding SHG properties of the water molecule. Below we proceed to discuss the consequences of describing water within the continuum, supermolecular, and semicontinuum models, and for notational convenience when listing tensor components, [*iij*] collectively designates (*iij*) and (*jii*).

Solvent Shifts for $\boldsymbol{\beta}$. From Tables 1 and 2 the solvent shifts in $\boldsymbol{\beta}$ due to the equilibrium ($\epsilon = 78.54$ entry) and nonequilibrium ($\epsilon_{st} = 78.54$ and $\epsilon_{op} = 1.78$ entry) continuum solvation model

are seen by comparing with the corresponding gas-phase numbers ($\epsilon = 1.00$ entry). The continuum model gives a positive solvent shift for β_{zzz}, which practically amounts to a sign change for this component, both within the equilibrium and nonequilibrium models. The solvent shifts for $\beta_{[xxz]}$ consist of a slight decrease for equilibrium solvation, whereas nonequilibrium solvation gives rise to an increase. Also $\beta_{[yyz]}$ are increased due to solvation, the shifts being most pronounced for equilibrium solvation.

Modeling solvation in the supermolecular approach leads to large solvent shifts in $\boldsymbol{\beta}$, as confirmed by comparing the $\epsilon = 1.00$ entries in Tables 1 and 3, and in Tables 2 and 4. Positive shifts in β_{zzz} and $\beta_{[xxz]}$ are in the range of 4 and 5 au, respectively, and as for the continuum model β_{zzz} undergoes a sign change. In particular, the supermolecular approach has a pronounced impact on $\beta_{[yyz]}$. For the EO effect $\beta_{[yyz]}$ are shifted positively about 8 au and for SHG around 8−10 au. At high frequencies β_{yyz} further has its sign changed by virtue of the first solvation shell. Employing the semicontinuum description for solvation leads to all positive components of $\boldsymbol{\beta}$, be it equilibrium or nonequilibrium solvation, as seen from either of the solvation entries of Tables 3 and 4. Solvent shifts of up to ∼13 au for the EO and ∼17 au for SHG effect are seen for the β_{zzz} component. Unlike the continuum description as applied to the water monomer, the semicontinuum model leads to large increases in $\beta_{[xxz]}$, in both the equilibrium and nonequilibrium model: around 7−8 au for the EO and 7−11 au for the SHG effect. By far the largest solvent shifts seen in this study occur for $\beta_{[yyz]}$. For SHG shifts are as large as ∼19 au, and again the shifts for nonequilibrium solvation are slightly moderated relative to those of equilibrium solvation.

The relative solvent shifts may be analyzed building the solvent environment in the following two ways: (gas phase → continuum model) and (gas phase → supermolecule → semicontinuum model). In the latter sequence we notice how especially $\beta_{[yyz]}$ are shifted positively by addition of a first solvation shell. From Figure 1 we see that the central water molecule is more hydrogen-bonded in the *yz*-plane which may explain that $\beta_{[yyz]}$ components are shifted more than $\beta_{[xxz]}$ components. The fact that β_{zzz} is less shifted may also be understood in this view, i.e., less interaction with the first solvation shell along the *z* direction. The next step, i.e., taking the supermolecule into the continuum description (the semicontinuum model) gives large positive shifts in β_{zzz} and in $\beta_{[xxz]}$. Thus, within the semicontinuum model $\beta_{[yyz]}$ are most susceptible to the short-range interactions, and β_{zzz} and $\beta_{[yyz]}$ most susceptible to long-range interactions. Conversely, solvating by means of the continuum model, $\beta_{[yyz]}$ components become the least shifted, with the additional feature that the sign of the shift differs for equilibrium and nonequilibrium approach.

Kleinman Splittings. Having the entire $\boldsymbol{\beta}$ tensor available, the previous assumption of Kleinman symmetry[5] is not required to evaluate $\beta_{||}$ and we may inquire on the validity of the assumption. From Tables 1 and 2 it is seen that $\beta_{[xxz]}$ differ by at most ∼2% in the gas phase. With equilibrium or nonequilibrium continuum solvation this symmetry is brought almost to perfection. From Tables 3 and 4, however, it is evident that a first solvation shell breaks this symmetry because $\beta_{[xxz]}$ components may differ by almost a factor of 2. Moving to the semicontinuum description, the Kleinman splitting of $\beta_{[xxz]}$ prevails. For $\beta_{[yyz]}$ Kleinman symmetry does not hold, neither in the gas phase nor in the continuum model, as evident from Tables 1 and 2. With the supermolecular description Kleinman splitting is decreased for the $\beta_{[yyz]}$ components, which differ by at most ∼7%, a trend present also within the semicontinuum model.

Hence, as we move from continuum to semicontinuum solvation, it seems that the Kleiman splitting is shifted from the $\beta_{[yyz]}$ to the $\beta_{[xxz]}$ components and, consequently, that overall Kleinman symmetry does not hold in any of the solvent models employed.

Dispersion of $\boldsymbol{\beta}_{||}$ and Comparisons with Experiment. The dispersion of $\beta_{||}$ within the different solvent models is displayed in Figures 2 and 3. The EO and SHG effect show quite similar trends, the differences arising mainly through an enhanced dispersion for $\beta_{||}^{2\omega}$ at high frequencies. As established previously,[21,5] the gas-phase water molecule has a negative β response, the magnitude of which increases with frequency. Differences in dispersion between $\beta_{||}^{2\omega}$ and $\beta_{||}^{\omega}$ amount at most to ∼20%. From Figure 3 it is clear that our gas-phase results for $\beta_{||}^{2\omega}$ are a factor of 2 lower than the experimental values due to Ward et al.[2] and Kaatz et al.[22]

In Figures 2 and 3 we see that continuum solvation makes $\beta_{||}$ increase, the negative sign being preserved, however, and that nonequilibrium solvation gives a slightly larger shift. Equilibrium and nonequilibrium solvation give almost identical dispersions, less pronounced, however, compared to the gas-phase result. From the experimentally based estimate of $\beta_{||}^{2\omega}$ shown in Figure 3 due to Levine et al.[1] the continuum model does not even qualitatively reproduce experiment as previously established.[10] Employing the supermolecular model positively shifts $\beta_{||}$ to nearly constant values between 5 and 6 au with a dispersion amounting to no more than ∼15% for the SHG case. The effect of a first solvation shell is therefore clear: $\beta_{||}$ changes sign and thus about a factor of 2 from reproducing the experimental estimate of $\beta_{||}^{2\omega}$. Adopting the semicontinuum approach induces positive solvent shifts as large as ∼27 au and ∼22 au for $\beta_{||}^{2\omega}$ and $\beta_{||}^{\omega}$, respectively. Equilibrium solvation induces a shift about 3 au larger than nonequilibrium solvation, and dispersions amounts to ∼10% for $\beta_{||}^{\omega}$ and ∼40% for $\beta_{||}^{2\omega}$. From Figure 3 we clearly see that semicontinuum solvation, in both the equilibrium and nonequilibrium approach overshoots the experimental value of the liquid-phase experiment.

Discussion

The results for $\beta_{||}^{2\omega}$ confirm the previous finding, i.e., that the sign change of the dipolar SHG response of water on liquefaction is reproduced using the supermolecular and semicontinuum models. The same conclusion may qualitatively be arrived at from the $\beta_{||}^{\omega}$ results as previously done. The continuum model does not give the sign change and the gas-phase values for $\beta_{||}^{2\omega}$ are a factor of 2 off the experimental estimate. The latter is clearly due to the lack of electron correlation, which may as much as double $|\beta_{||}^{2\omega}|$,[5,10,11,13,21,23,24] and the use of a limited basis set. In the continuum model, electron correlation increases the magnitude of $\beta_{||}$ [5,10,11] and therefore cannot explain the wrong sign obtained for $\beta_{||}^{2\omega}$. The influence of basis set is less clear but in ref 11 a sign change for $\beta_{||}^{2\omega}$ was seen in CC2 and CCSD continuum calculations as the basis set size was increased. This could be due to the solute wave function leaking out into the dielectric medium, however.

Introducing a first solvation shell using the same basis set and identical orientation of the central monomer makes conclusions more firm than previously: $\beta_{||}$ does change sign and is within a factor of 2 of experiment. It must be stressed that the pentametric water cluster is a C_{2v} idealization and that spatial

changes of the local environment can have tremendous impact on $\beta_{||}$, even a sign change.[14] In a more rigorous approach one would clearly need to consider an ensemble of solvation shell configurations obtained from MD simulations and make the appropriate statical averaging. Also, it is by no means obvious that the differential shell approach is appropriate for obtaining the monomer properties.

Adopting the semicontinuum model significantly increases $\beta_{||}$ and for $\beta_{||}^{2\omega}$ over shoots the liquid-phase estimate by Levine et al.[1] This latter number, however, should be questioned as it relies on doubtful estimates for the second hyperpolarizability ($\gamma_{||}^{2\omega}$) and dipole moment (μ) for water, and the use of local field factors in an inconsistent way.[25] Further, the quartz reference used in EFISH experiments has been updated[26] since then. Reinterpreting the measurement by Levine et al. with this in mind, a factor of 2 increase in the experimental estimate of $\beta_{||}^{2\omega}$ for water in the liquid phase can well be justified. In this perspective, the semicontinuum results for $\beta_{||}^{2\omega}$ appear satisfactory, although the scarcity of experimental data (one experiment) makes firm conclusions impossible.

The common assumption of Kleinman symmetry was shown not to hold in any of the investigated solvation schemes, although splittings occur less pronounced in the semicontinuum model. This might be attributed to the larger degree of spherical symmetry of the pentamer relative to the monomer. This also raises the issue of analyzing the optical characteristics of liquid water in terms of monomer properties. Alternatively, the pentamer unit could be considered the smallest representable unit to mimic the associated nature of the liquid phase.

Acknowledgment. We thank J. Kongsted for helpful discussions and suggestions in the preparation of this paper. K.V.M. thanks Statens Naturvidenskabelige Forskningsråd, Statens Teknisk Videnskabelige Forskningsråd, Danish Center for Scientific Computing, and the EU networks MOLPROP+THEONET II and NANOQUANT for support.

References and Notes

(1) Levine, B. F.; Bethea, C. G. *J. Chem. Phys.* **1976**, *65*, 2429.
(2) Ward, J. F.; Miller, K. *Phys. Rev. A* **1979**, *19*, 826.
(3) Kaatz, P.; Donley, E. A.; Shelton, D. P. *J. Chem. Phys.* **1998**, *108*, 849.
(4) Willetts, A.; Rice, J. E.; Burland, D. M. *J. Chem. Phys.* **1992**, *97*, 7590.
(5) Mikkelsen, K. V.; Luo, Y.; Ågren, H.; Jørgensen, P. *J. Chem. Phys.* **1995**, *102*, 9362.
(6) Narten, A. H. *J. Chem. Phys.* **1971**, *55*, 2268.
(7) Mikkelsen, K. V.; Jørgensen, P.; Jensen, H. J. Aa. *J. Chem. Phys.* **1994**, *100*, 6597.
(8) Mikkelsen, K. V.; Cesar, A.; Ågren, H.; Jensen, H. J. Aa. *J. Chem. Phys.* **1995**, *103*, 9010.
(9) Mikkelsen, K. V.; Sylvester-Hvid, K. O. *J. Phys. Chem.* **1996**, *100*, 9116.
(10) Sylvester-Hvid, K. O.; Mikkelsen, K. V.; Jonsson, D.; Norman, P.; Ågren, H. *J. Chem. Phys.* **1998**, *109*, 5576.
(11) Kongsted, J.; Osted, A.; Mikkelsen, K. V.; Christiansen, O. *J. Chem. Phys.* **2003**, *119*, 10519.
(12) Poulsen, T. D.; Ogilby, P. R.; Mikkelsen, K. V. *J. Chem. Phys.* **2001**, *115*, 7843.
(13) Jensen, L.; van Duijnen, P. Th.; Snijders, J. G. *J. Chem. Phys.* **2003**, *118*, 514.
(14) Reis, H.; Raptis, S. G.; Papadopoulos, M. G. *Chem. Phys.* **2001**, *264*, 301.
(15) Reis, H.; Papadopoulos, M. G.; Theodorou, D. N. *J. Chem. Phys.* **2001**, *114*, 876.
(16) Gubskaya, A. V.; Kusalik, P. G. *Mol. Phys.* **2001**, *99*(13), 1107.
(17) Almlöf, J.; Taylor, P. R. *J. Chem. Phys.* **1987**, *86*, 4070.
(18) Jorgensen, W. L.; Chandrasekhar, J.; Madura, J. D.; Impey, R. W.; Klein, M. L. *J. Chem. Phys.* **1983**, *79*, 926.
(19) Rahman, A.; Stillinger, F. H. *J. Am. Chem. Soc.* **1973**, *95*, 7943.
(20) Geiger, A.; Stillinger, F. H.; Rahman, A. *J. Chem. Phys.* **1979**, *74*, 4185.
(21) Luo, Y.; Ågren, H.; Vahtras, O.; Spirko, V.; Jørgensen, P.; Hettema, H. *J. Chem. Phys.* **1993**, *98*, 7159.
(22) Kaatz, P.; Donley, E. A.; Shelton, D. P. *J. Chem. Phys.* **1998**, *108*, 849.
(23) Sekino, H.; Bartlett, R. J. *J. Chem. Phys.* **1993**, *98*, 3022.
(24) Dalskov, E. K.; Jensen, H. J. Aa.; Oddershede, J. *Mol. Phys.* **1997**, *90*, 3.
(25) Macak, P.; Norman, P.; Luo, Y.; Ågren, H. *Chem. Phys.* **2000**, *112*, 1868.
(26) Kaatz, P.; Shelton, D. P. *J. Chem. Phys.* **1996**, *105*, 3918.